4.1 # AN EXPLANATION OF ACTINIAE CLOUD PATTERNS

ERNEST M. AGEE*
DEPARTMENT OF EARTH AND ATMOSPHERIC SCIENCE, PURDUE UNIVERSITY

1. INTRODUCTION

The author was inspired to address this subject on the basis of the recent article by Garay et al. (2004) that presented a remarkable new collection of actiniae cloud patterns, as observed from space. The primary objective of this paper is to present a more collective view of the fluid dynamics of actiniae convection, and to offer new physical insight as to the nature and cause of actiniae clouds. Beautiful observations of actiniae and their behavior have been provided by the Space Science and Engineering Center, University of Wisconsin-Madison, (http://cimss.ssec.wisc. edu/wxwise/swirl/actinae2.htm). Please note that actiniae is misspelled in the website address. The late Lester F. Hubert from the Meteorological Satellite Laboratory, NOAA, was an invited speaker at NCAR's 1966 Summer Colloquium on "Thermal Convection." The author was in attendance and became inspired by Hubert's lectures and personal exchanges regarding cloud observation from space platforms. Also, at that time, the late Walter Orr Roberts, upon visiting the Soviet Union, returned with COSMOS satellite images of actiniae cloud patterns that were given to the author (through the courtesy of V. A. Bugaev). For over 40 years we have observed actiniae clouds, and to a large extent they have been ignored, and certainly not adequately explained. Agee (1984) published a NIMBUS I image of actiniae off the coast of Peru on 15 September 1964. He noted that the actiniae tend to be located over cool ocean currents, and generally between regions of open and closed mesoscale cellular convection (MCC). Agee (1987) defines and discusses the Type I and Type II cloud-topped boundary layers (CTBLs) associated respectively, with the wintertime and summertime cloudy marine boundary layers over warm and cool ocean currents. An updated climatology of the Type I and Type II MCC is presented in Fig. 1. Actiniae are never found in wintertime Type I CTBLs, but are frequently seen in the summertime Type II CTBLs over cool ocean currents. Type I systems are more dynamic, driven by heating from below; while Type II systems are more lethargic and are driven from above by radiative-entrainment effects. The author now understands that the "defects" in Type II cloud events (for example, see Fig. 5 in Agee 1987) often seen in GOES imagery, are most likely to have the same detail as evident in higher resolution photographs taken by astronauts (e.g., see Fig. 2 in Garay et al. 2004). It can be noted in general that the actiniae structure represents a breakdown from the more common cellular pattern, and a collective imbalance of forces or physical processes responsible for the convection leads to a new geometry. Agee (1999) in an address at the AMS meetings in Dallas discussed the relevance of *Le Chatelier's Principle* to such meteorological events (namely, "any inhomogeneity that somehow develops in a system should induce a process that tends to eradicate the inhomogeneity"). The author chooses to name the meteorological version of *Le Chatelier's Principle* for convection, the *Principle of Efficiency*. When the state of existence of any system is "stressed" (e.g., a fluid at rest if uniformly and sufficiently heated, will overturn, creating a preferred convective geometry such as Benard cells) it can ultimately readjust to the new conditions and it will do so in the most efficient way (whether responding to heat transfer, wind shear, rotation, surface tension on a free surface, or a host of imaginable processes). Before leaving the introduction, it is interesting to note that the root word for naming actiniae clouds is of Greek origin, *anemone*, which refers to plants/animals with radial extensions such as tentacles and arms. The *Sea Anemone* is appropriately named (the home of Nemo), as well as the cup anemometer. Actinia is singular, the word actiniae is plural, and *actiniae clouds* are clouds with radial arms of convective structure.

2. THE THEORY AND GEOMETRY OF LABORATORY THERMAL CONVECTION AND ACTINIAE

Laboratory examples of thermal convection geometry cover an uncanny range of structures. As noted by Agee (1999) this varies from the more common 2-d rolls and 3-d cells, to a

**Corresponding author address:* Ernest M. Agee, Purdue University, Dept. of Earth and Atmospheric Sciences, 550 Stadium Mall Drive, West Lafayette, IN 47907-2051; e-mail: eagee@purdue.edu.

litany of structures listed in Table 1. Conditions and/or properties known to affect convective structure are also presented in Table 1. It is possible to write your name in convection, but for the purposes of this paper the classical view is taken of uniform heating from below and/or cooling from above. A regime stability diagram of Rayleigh Number (Ra) versus Prandtl Number (Pr) for laboratory experiments is presented in Fig. 2, taken from Krishnamurti (1975a). Experiments in mercury, air, water, oils, etc. show that the preferred onset geometry of convective structures (for a thermally unstable fluid layer) is 2-d bands. Further increases in Ra can transform the steady 2-d bands into steady 3-d hexagons (actually three families of lines oriented respectively at 60° angles to one another), and ultimately into time dependent cross-modal flows of various irregular shapes. Krishnamurti also introduces a vertical asymmetry parameter, called γ, to represent another physical process that is capable of altering the onset conditions for convection and the geometric shape. Figure 2 therefore represents the $\gamma = 0$ plane, while Fig. 3 shows Krishnamurti's new regime stability diagram for an imposed constant background vertical velocity. Krishnamurti (1975a, b) showed theoretically and experimentally that large-scale up motion produces "up hexagons" or closed cells, while large-scale down motion produces "down hexagons" or open cells (also see Agee et al. 1973). It is further noted that the condition of $\gamma \neq 0$ changes the onset geometry from 2-d rolls (in the $\gamma = 0$ plane) to a 3-d regular array of hexagons. Agee and Chen (1973) have also discussed another γ factor, namely the vertical variation of turbulent viscosity effects, which can increase or decrease with height. This is analogous to the original work by Palm (1960) that shows the theoretical role of molecular viscosity variations as a function of temperature, which increases with height in liquids (yielding closed cells) and decreases with height in gases (yielding open cells).

2.1 The Regime-Stability Diagram for Convective Marine PBLs

Nature's laboratory for convective overturning of a fluid layer is best achieved over the oceans where more uniform conditions can prevail, which approximate those for Rayleigh-Benard (RB) convection. As noted earlier, this is achieved by heating from below (cold air over warm water), or by cloud top radiative-entrainment processes (with no temperature difference between the air and sea surface). Figure 4 is a proposed conceptual diagram of the atmospheric version of the classical regime stability diagram for thermal convection. Rolls, cells, actiniae, time-dependent cross-modal structures and various types of irregular geometry are allowed (and observed) within convective marine PBLs. However, the atmospheric equivalents of Ra and Pr are not well understood or defined. Krishnamurti (1975a) has provided an insightful discussion of a possible range of Pr_{atm} from 1 to 50, which is well beyond the molecular value for air (Pr = 0.7). This larger range of proposed Pr_{atm} is very significant, allowing consistency between the regime stability diagrams presented in Figs. 2 and 4, thereby not restricting the events to the small domain of a small Pr. Another similar fluid dynamics instability phenomenon can be seen in von Kármán vortex streets created in the laboratory versus the atmosphere. Agee (1975) and Jensen and Agee (1978) have noted such comparisons, and these studies have argued successfully the effective viscosity required in the atmosphere to produce such vortex patterns and shedding frequency (based on the relationship between the Reynolds Number and the Strouhal Number). More recent similar findings have been reported by DeFelice et al. (2000). In recent discussion between Peter Sullivan and the author, it was readily agreed that von Kármán vortex streets and thermal convection (and associated geometry) are all embedded in the Navier-Stokes equations. The difficulty is determining the appropriate non-dimensional numbers for atmosphere flows, such as Ra_{atm}, Pr_{atm}, and Re_{atm}.

2.2 Thermal Convection in Ethanol and Vegetable Oil with Radial Patterns

The creation of radial arms of convective structure in laboratory cells can be readily achieved (as evident in the results reported below). Krishnamurti (1975a) showed the role played by the Ra in determining the radial structure of cells. At weak supercritical Ra ($\approx Ra_c$) she developed a pattern of hexagons with six arms, extending from cell center to each vertex. As the Ra was increased to 10 Ra_c, the nonlinear terms in the Boussinesq equations produced a second set of arms extending from cell center, perpendicular to each side (for a total of 12 arms). Further increases in the Ra can cause irregular geometry and cell lengthening with a multitude of time dependent radial structures. This is illustrated in Fig. 5, for an irregular pattern of cells in ethanol (CH3-OH) for conditions of depth = 0.56 cm, T_{bot} = 25.8°C and T_{top} 20.8°C (photo provided through the courtesy of F. H. Busse). The convective cells in Fig. 5 could appropriately be labeled as "laboratory actiniae."

Another laboratory experiment was conducted by the author for vegetable oil, with Pr = 800 and Ra values up to 320,000 (~300 Ra_c) for rigid-free boundary conditions. Depth was fixed at 2 cm and ΔT across the layer was up to 4.5C°cm^{-1}, with uniform heating from below. Visualization was achieved by adding neutrally buoyant flakes of molybdenum disulfide to the vegetable oil. Weak supercritical conditions achieved results similar to that observed by Krishnamurti, and larger supercritical conditions obtained results as observed by Busse. Figure 6 shows the "defect" pattern of an actiniae cell at ~ 300 x Ra_c. As noted earlier, actiniae occupy a small domain in the regime stability diagram for thermal convection, and it is not easy to achieve this cloud pattern in the atmosphere (and to a certain extent in the laboratory as well). Figure 7 shows an actinia cell over the eastern North Pacific on 17 June 1997 (see http://cimss.ssec.wisc.edu/wxwise/swirl/actinae2.htm).

No precise laboratory patterns of actiniae have been developed under conditions of velocity shear, but it is reasonable to assume that lengthy 2-d and 3-d chains of actiniae-like structure could be produced (analogous to the images referenced earlier in Garay et al. 2004). In the real atmosphere, varying degrees of wind shear could produce such an elongating effect or string of actiniae. The presence of vertical vorticity can also produce rotation, with individual actinia displaying a rotor type of appearance for the convective arms (see time loops of such features at the University of Wisconsin, SSEC, website presented earlier).

3. SUMMARY AND CONCLUSIONS

Actiniae cloud patterns can be viewed as a natural feature or atmospheric manifestation of RB convection, which has been successfully studied both theoretically and experimentally in the laboratory. The subtle radial arms of convection cells at weak supercritical Ra become more numerous and distinctive as the Re increases to moderately large supercritical values. It is further noted that the actinia structure is not a commonly preferred geometry, and the author has elected to refer to such structure as a "defect" when the cell appears within a pattern of mesoscale cellular convection over the ocean. The MCC pattern is not expected over land, where homogeneous boundary conditions of heating are unlikely. Further, the domain of the actinia structure on a regime stability diagram for thermal convection is viewed as somewhat limited, and characterized by a small range of Pr_{atm} and Ra_{atm} conditions. This further supports the more common observation of actiniae in Type II convective marine PBLs and never in the Type I convective marine boundary layers. Precise values for Ra_{atm} and Pr_{atm} (as well as Re_{atm}) continue to challenge the thinking of atmospheric dynamicists who believe that MCC, vortex streets in the wake of islands, actiniae, etc. have theoretical understanding embedded in the Navier-Stokes Equations.

4. ACKNOWLEDGEMENTS

The author is grateful to Brooke Halvorson for assisting with convection experiments in vegetable oil; and Gina Richey for technical assistance with the manuscript. Mark and June Chen are respectfully acknowledged for financial contributions to Purdue University in support of this work, as well as NSF Grant ATM-0514674 awarded to Purdue University.

5. REFERENCES

Agee, E. M., 1975: Some inferences of eddy viscosity associated with instabilities in the atmosphere. *J. Atmos. Sci.*, **32**, 642-646.

———, 1984: Observations from space and thermal convection: A historical perspective. *Bull. Amer. Meteor. Soc.,* **65**, 938–949.

———, 1987: Mesoscale cellular convection over the oceans. *Dyn. Atmos. Oceans*, **10**, 317-341.

———, 1999: 2-d or not 2-d: That is the question. *13th Symposium on Boundary Layers and Turbulence*, Dallas, TX, Amer. Meteor. Soc., 123-126.

———, and T. S. Chen, 1973: A model for investigating eddy viscosity effects on mesoscale cellular convection. *J. Atmos. Sci.*, **30**, 180–189.

———, ———, and K. E. Dowell, 1973: A review of mesoscale cellular convection. *Bull. Amer. Meteor. Soc.*, **54**, 1004–1012.

DeFelice, T. P., D. J. Meyer, G. Xian, J. Christopherson, and R. Cahalan, 2000: Commentary and Analysis: Comments on Landsat-7 Reveals More Than Just Surface Features in Remote Areas of the Globe. *Bull. Amer. Meteor. Soc*., **81**, 1047-1049.

Garay, M. J., R. Davies, C. Averill, and J. A. Westphal, 2004: Actinoform clouds: Overlooked examples of cloud self-organization at the mesoscale. *Bull. Amer. Meteor. Soc*., **85**, 1585-1594.

Jensen, N. O., and E. M. Agee, 1978: Vortex cloud street during AMTEX 75. *Tellus*, **30**, 517-523.

Krishnamurti, R., 1975a: On cellular cloud patterns-Part 1: Mathematical model. *J. Atmos. Sci.,* **33**, 1353-1363.

———, 1975b: On cellular cloud patterns. Part 2: Laboratory model. *J. Atmos. Sci.,* **32**, 1364–1372.

Palm, E., 1960: On the tendency toward hexagonal cells in steady convection. *J. Fluid Mech*., **8**, 183-192.

Table 1. Convection Geometry and Conditions/Properties that affect convective shapes.

a. Geometric Shapes

2-d rolls	herring-bone
3-d cells	6-arm hexagons
chains/beads	12-arm hexagons
bi-modal	skewed varicose
cross-modal	knot
actinia	zigzag
pan-am	spiral rotors
spiral defect	vortices at vertices
non-defect spiral	turbulent
bi-harmonic	slime mold
spoke-pattern	(etc.)
oscillatory	

b. Conditions/Properties

at rest	no Hadley mode
motion	subcritical Re
lateral boundaries	supercritical Re
infinite boundaries	weak supercritical Ra
constant physical properties	moderate supercritical Ra
variable physical properties	large supercritical Ra
motion (no shear)	radiative-entrainment
motion (with shear)	gravity waves
rotation	surface tension
no rotation	(etc.)
Hadley mode	

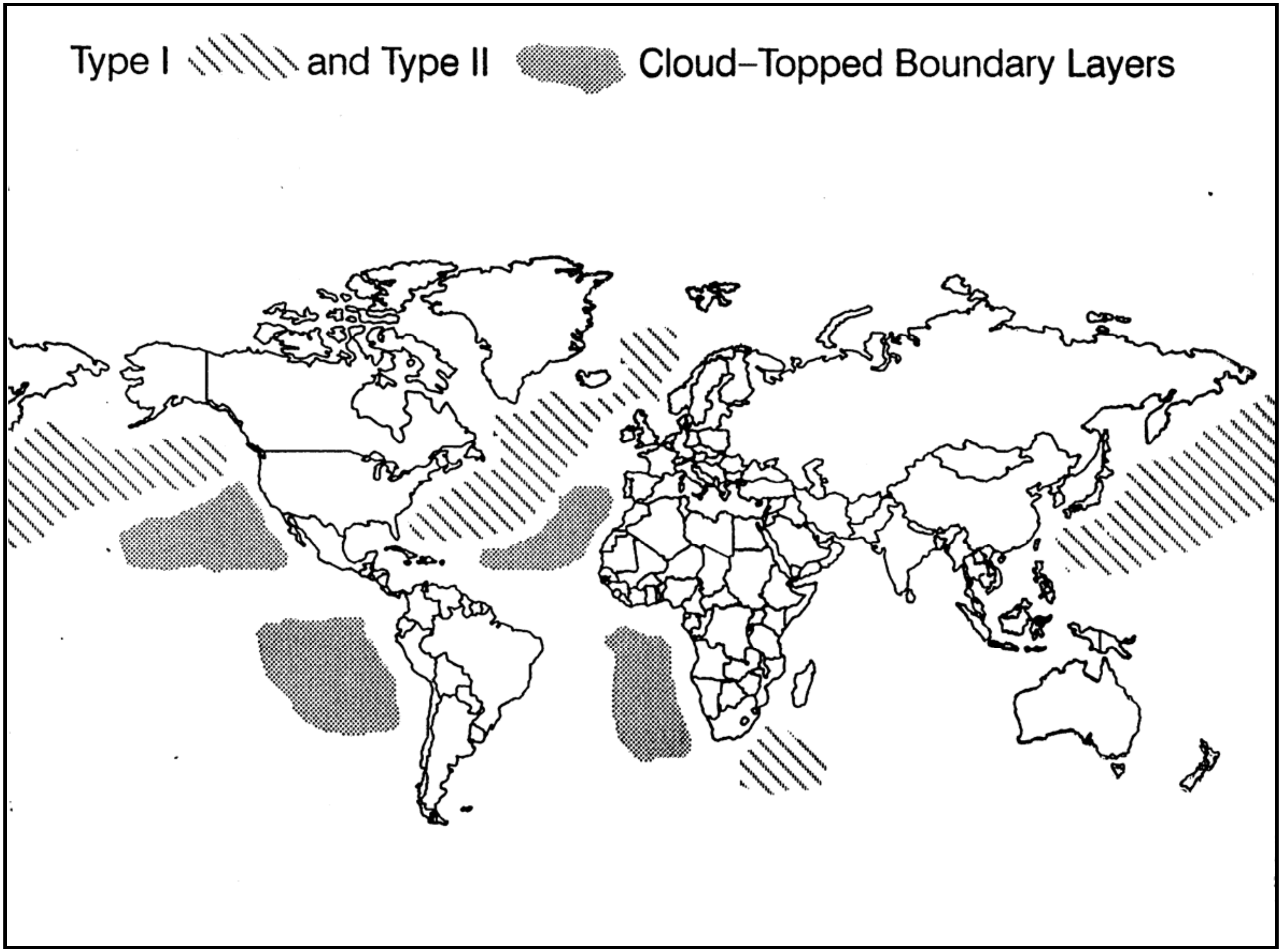

Figure 1. A global climatology of Type I and Type II CTBLs (see Agee 1984, 1987).

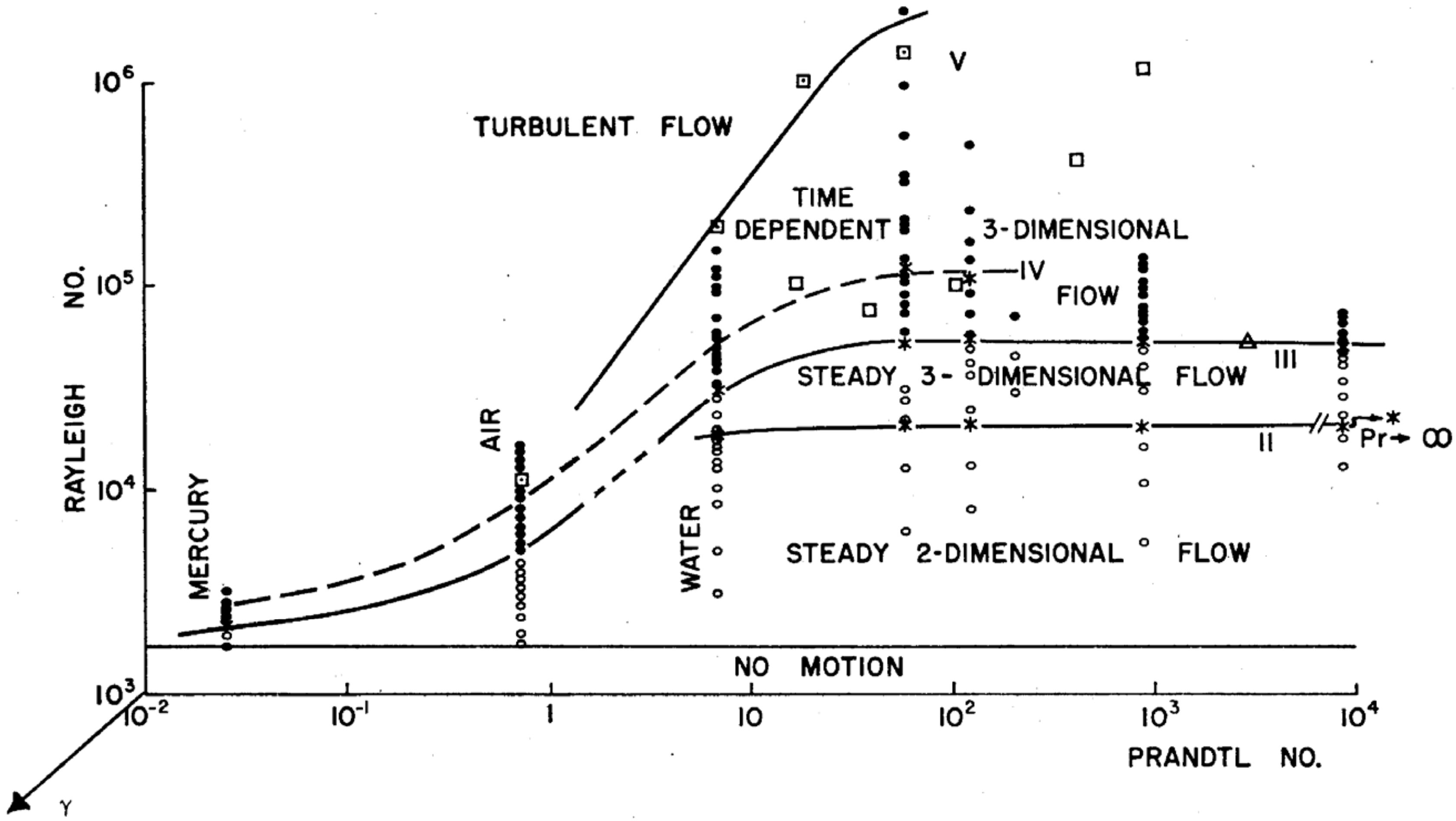

Figure 2. Experimental regime stability diagram for thermal convection, with observed convective structures (after Krishnamurti 1975a). γ is an imposed asymmetry representing an additional physical process.

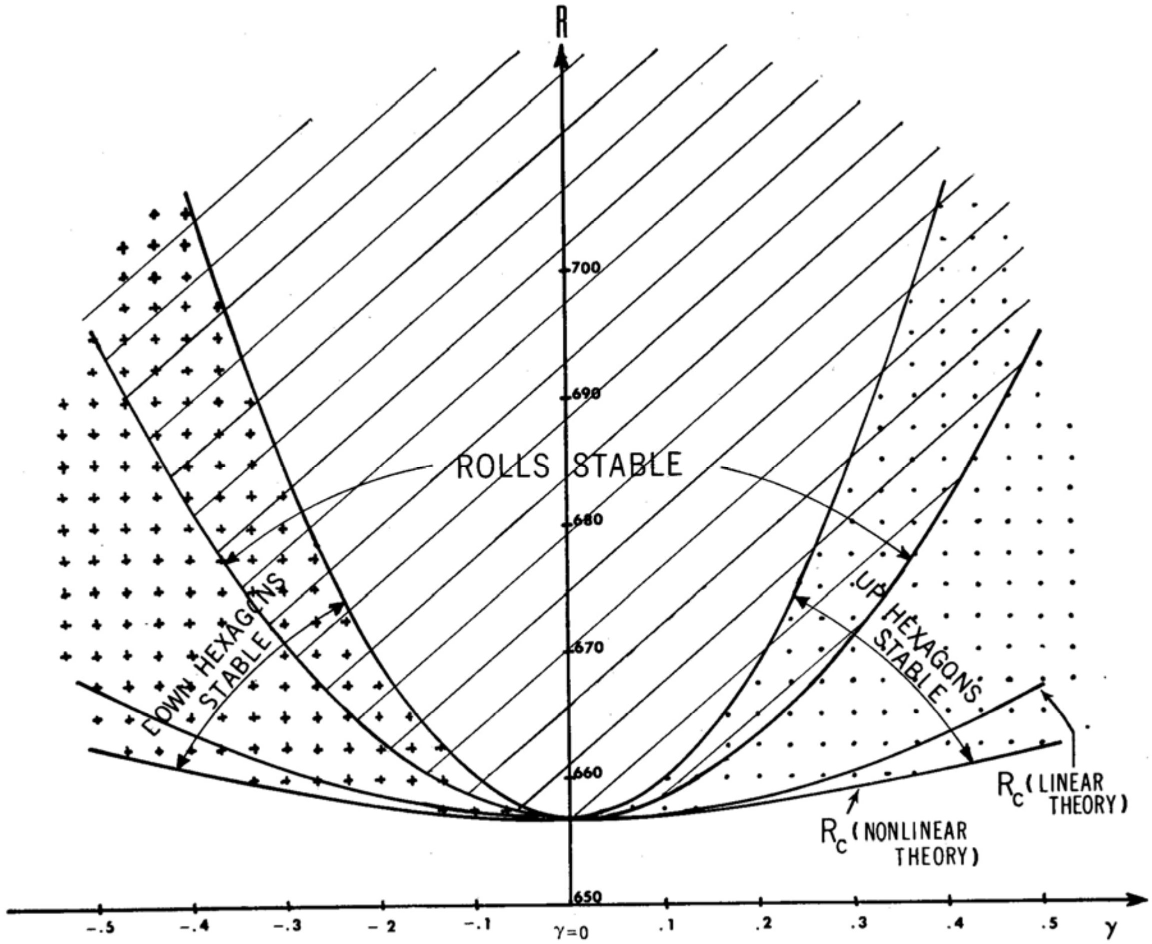

Figure 3. The regime-stability diagram for thermal convection under conditions of weak supercritical Ra, with large-scale up motion ($\gamma > 0$) or large-scale down motion ($\gamma < 0$), after Krishnamurti (1975a).

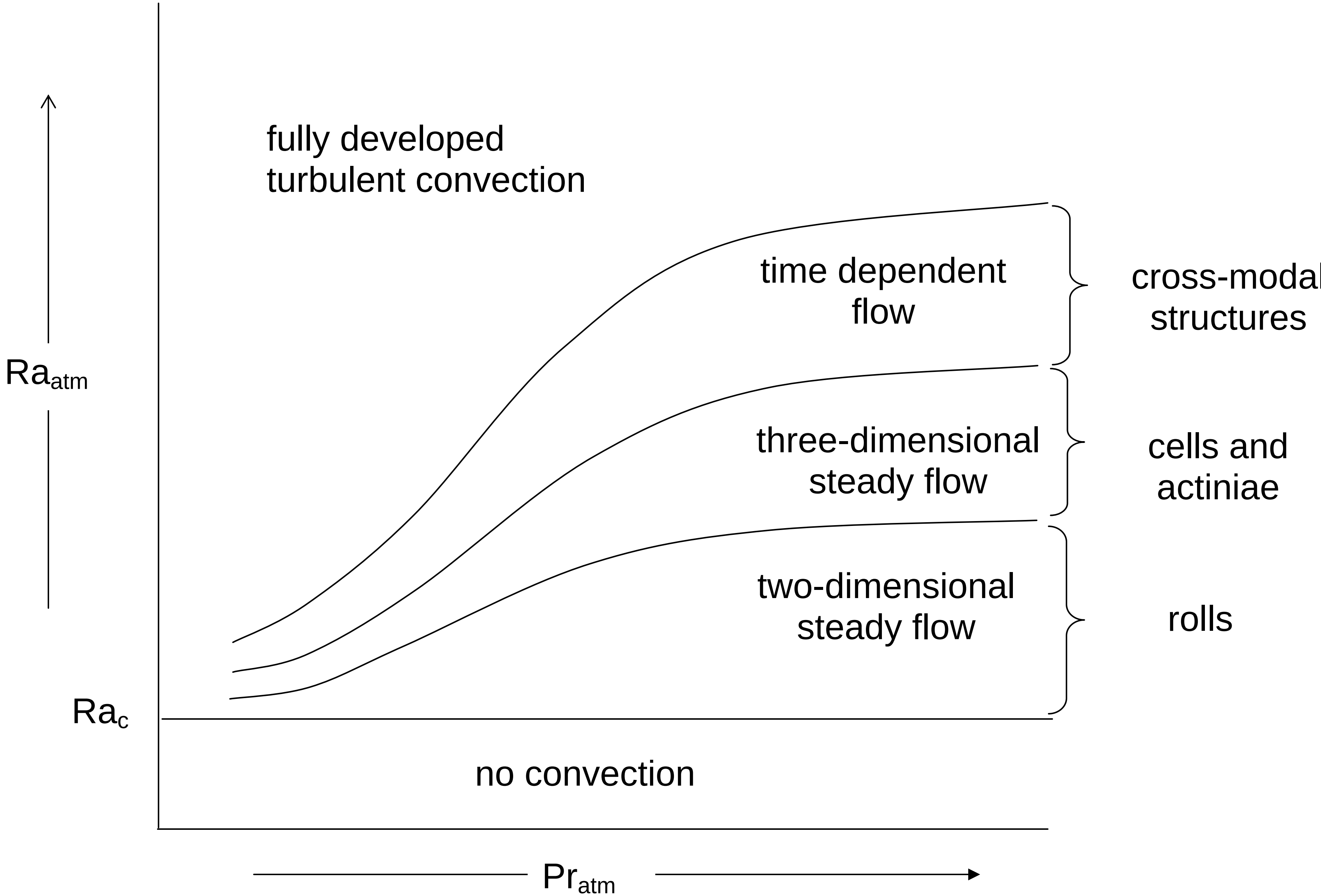

Figure 4. A conceptual regime stability diagram for cloud geometry in convective marine boundary layers.

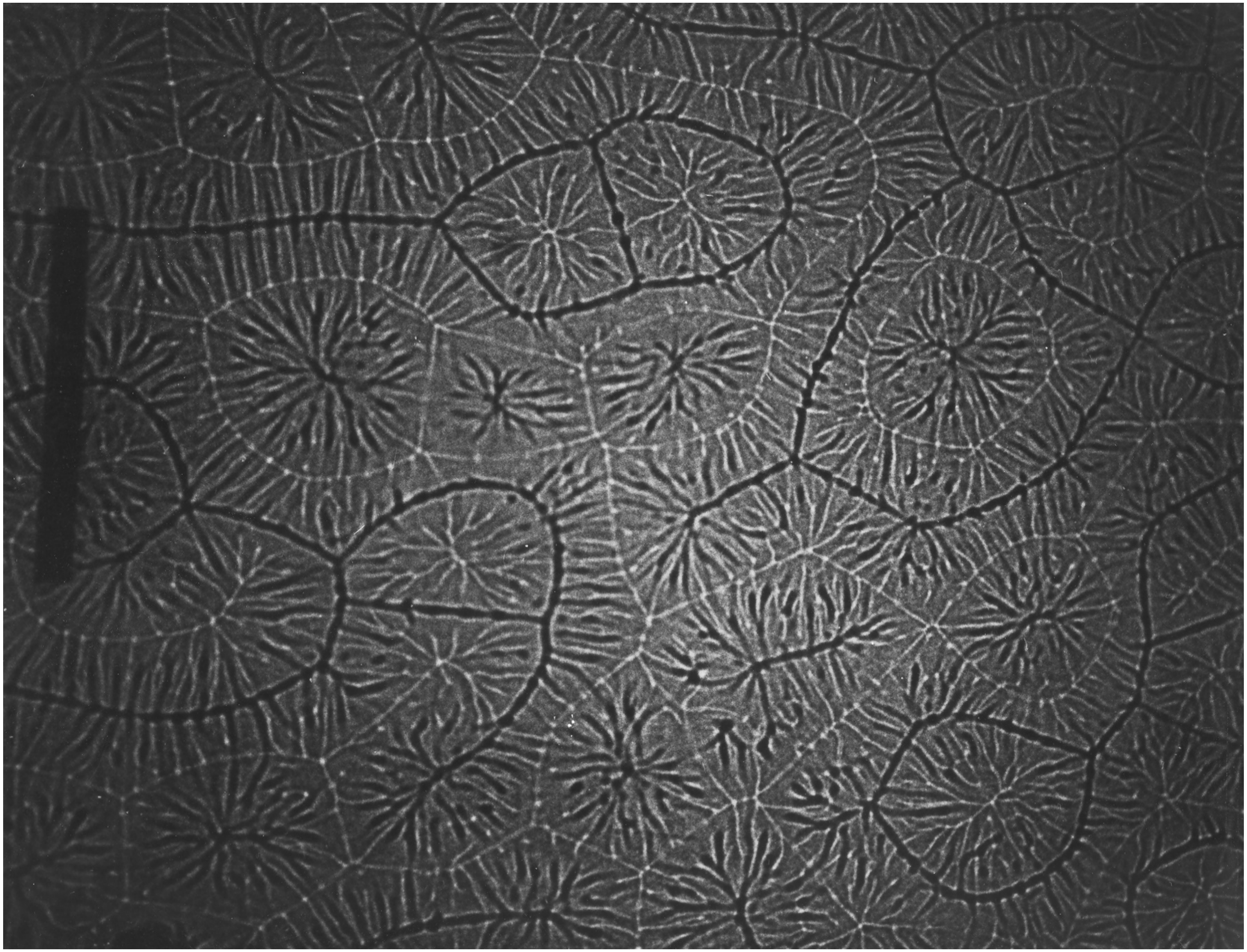

Figure 5. Laboratory convection cells in ethanol (CH3-OH), with actiniae structures (photo, courtesy of F. H. Busse); depth = 0.56 cm and ΔT = (25.8°C - 20.8°C).

Figure 6. An actinia transition cell embedded in RB convection, formed in vegetable oil at Pr = 800 and Ra = 300 x Ra_c; depth = 2.0 cm and ΔT = (44.5°C - 40°C).

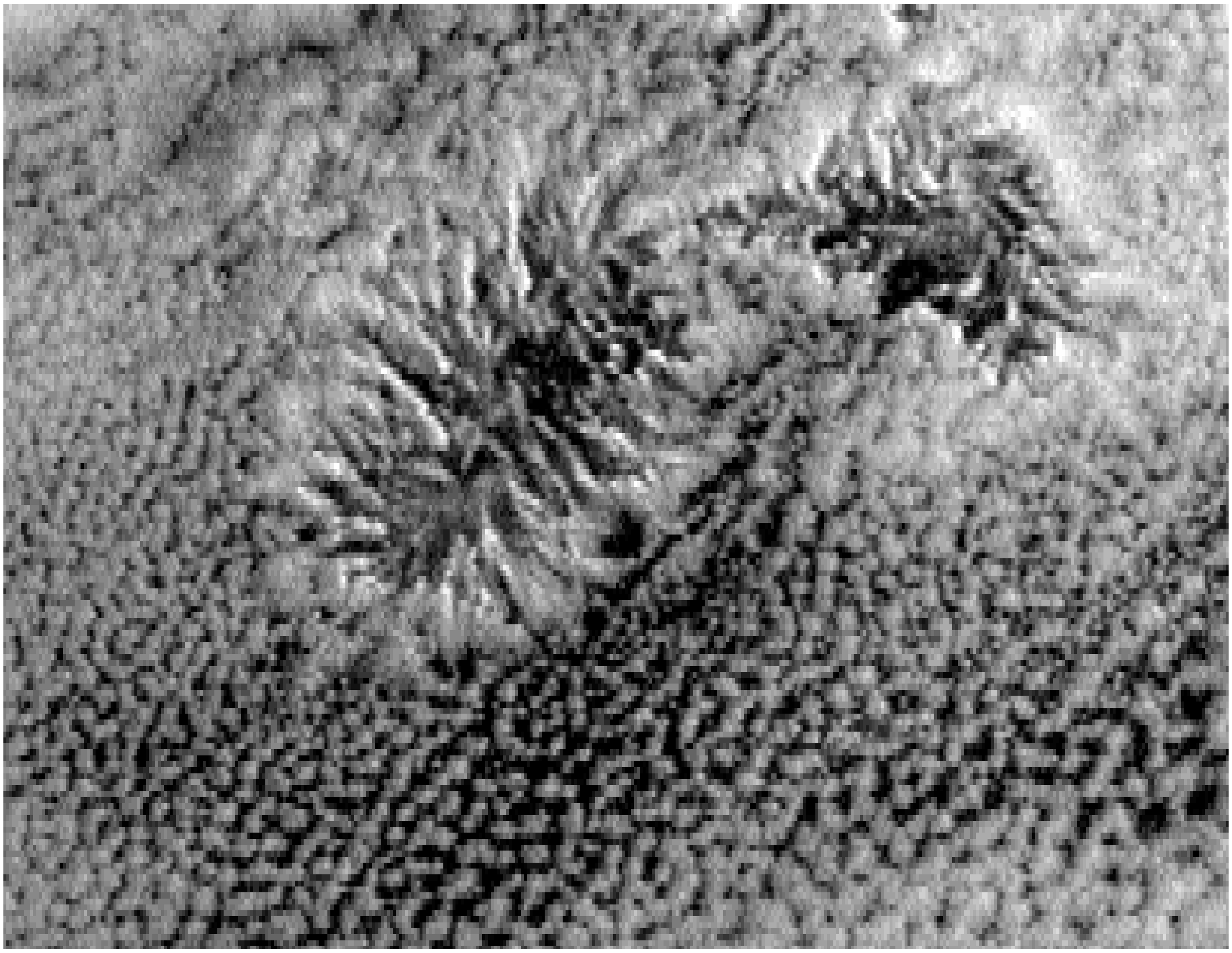

Figure 7. Transition (or defect) actiniae, embedded in mesoscale cellular convection over the eastern North Pacific on 17 June 1997 (see website at http://cimss.ssec.wisc.edu/wxwise/swirl/actinae2.htm).